

3D Modeling of Urban Tree Crown Volumes Using Multispectral LiDAR Data

Jonathan LI, Xinqu CHEN, Canada, Pengdi HUANG and Cheng WANG, China

Key words: Carbon Storage, Multispectral LiDAR data, Dendrometric Parameter Estimation, Tree Crown

SUMMARY

This paper presents a new method for quantifying the carbon storage in urban trees using multispectral airborne LiDAR data. Our method consists of four steps: multispectral LiDAR data processing, vegetation isolation, dendrometric parameters estimation, and carbon storage modeling. Our results suggest that LiDAR-based dendrometric parameter estimation and allometric models can yield consistent performance and accurate estimation. Citywide carbon storage estimation is derived in this paper for the Town of Whitchurch-Stouffville, Ontario, Canada by extrapolating the values within the study area to the entire city based on the specific proportion of each land cover type. The proposed method reveals the potential of multispectral LiDAR data in land cover mapping and carbon storage estimation at individual-tree level.

1. INTRODUCTION

Urban vegetation has drawn the direct attention of city planners and policy makers, considering the importance of trees in urban climate modification and energy conservation. In the context of Canada's climate, annual cooling energy use can be reduced 10-19% by planting vegetation proximate to the houses and increasing the albedo of urban surfaces (Xu et al., 2012; Sawka et al., 2013). City wide, urban trees reduce air pollution through direct dry deposition, and also influence the cooling of the ambient temperature, which slows smog formation. Vegetation contributes the largest proportion of carbon storage, which in return reduces the rate of climate warming and urban heat islands (Davies et al., 2011). Urban trees both sequester CO₂ and store excess carbon in biomass (71% of total urban carbon storage), which significantly influences environmental quality and human health (Donovan & Butry, 2011; Roy & Pickering, 2012). Preserving carbon storage and improving green space infrastructure in urban areas has significant environmental benefits (van den Berg et al., 2015). Consequently, estimation and monitoring of urban carbon stocks and green space becomes important indeed. In literature, the carbon content stored in individual trees can be assessed through aboveground dry-weight biomass calculation using allometric equations. Dendrometric parameters, such as individual tree height or crown diameters, are generally used in the allometric equations to derive diameter at breast height (DBH). Dry biomass is then calculated using the allometric model, with DBH as the input, and further transformed to carbon storage with a conversion rate around 0.5 (Lieth, 1963).



Fig. 1 Location of 40 sampled trees in the field

Airborne LiDAR has proven to be promising for the derivation of dendrometric parameters. Previous studies have shown that the LiDAR-derived canopy height model (CHM) has been used for dendrometric measurements and biomass estimation in urban studies (Huang et al., 2013; Raciti et al., 2014; Schreyer et al., 2014). Raciti et al. (2014) developed a LiDAR-height-only regression model to estimate carbon storage in urban trees across the city of Boston. A total of 404 accurately segmented tree crowns from the nDSM were split into 284 samples for model fitting and 120 samples for validation. The reason for using a simple linear regression of tree biomass and height was to avoid the influence of crown segmentation results. A R^2 of 0.79 was found between field-estimated biomass and model-predicted biomass. Schreyer et al. (2014) estimated the carbon storage in urban trees, and its distribution was extrapolated to the entire city of Berlin in terms of land use types. This study did not propose a region-specific allometric model for the study area, but applied the LiDAR-DBH model developed by Zhao et al. (2009) and a carbon allometric model using DBH as the only independent variable. 87% of the modeled DBH showed an underestimation, which was further calibrated by a weighted arithmetic average DBH. The carbon storage in urban trees was calculated as half of the model-based biomass, regardless of the genus. Meanwhile the crown base height was assumed to be half of the LiDAR-derived height, and the crown width was calculated in 16 directions with a series of criteria, instead of the conventional estimation of crown width in 4 directions (Popescu et al., 2003; Xu et al., 2014).

With the emerging multispectral LiDAR with multiple laser channels (or mLiDAR), it became possible to obtain both the range and multiple reflectance data from a single data source. The first commercial mLiDAR system, Titan, released by Teledyne Optech Inc., has integrated three laser channels at wavelengths of 532 nm (green), 1064 nm (NIR), and 1550 nm (SWIR), respectively. These three channels produce independent scan lines by sending pulses with separate forward angles (the channels NIR, SWIR and green have forward angles 0° , 3.5° , and 7.0° , respectively). This emerging mLiDAR system showed great potential in land cover mapping without the aid of passive multispectral images (Wichmann et al., 2015). This active laser system can largely avoid those factors commonly associated with passive optical sensors, such as weather conditions and shadow effects. However, the potential of mLiDAR intensity currently remains undervalued, and

Table 1. Combinations of input data for SVM classification

Selection 1	Green + NIR + SWIR + nDSM + pNDWI + pNDVI
Selection 2	Green + NIR + SWIR + nDSM
Selection 3	NIR + nDSM

3D Modeling of Urban Tree Crown Volumes Using Multispectral LiDAR Data (8875)
Jonathan Li (China, PR) and Xinqu Chen (Canada)

FIG Working Week 2017

Surveying the world of tomorrow - From digitalisation to augmented reality

Helsinki, Finland, May 29–June 2, 2017

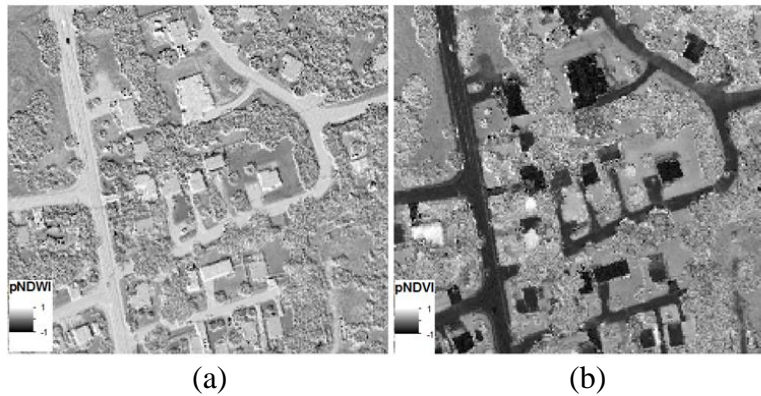


Fig. 2 Examples of LiDAR-intensity-derived indices

the applications of this newly released system are at an early stage of development.

Given the current state of development of tree inventory with single-channel conventional LiDAR data, this paper aims to explore the feasibility of mLiDAR range and intensity data in carbon storage estimation. To achieve this, vegetation covers are first classified based on mLiDAR range and intensity data by applying a Support Vector Machine (SVM) classifier. Secondly, dendrometric parameters such as tree height and crown diameter are derived, in order to establish an allometric relationship between LiDAR-derived measurements (tree height and crown diameter) and the field-measured parameter (DBH) through regression modeling. Lastly, this study quantifies the carbon storage in urban trees for the Town of Whitchurch-Stouffville, Ontario, Canada.

2. STUDY AREA AND DATASETS

Located in the Town of Whitchurch-Stouffville, Ontario, Canada, the study area is characterized by a typical residential landscape. It contains two water bodies (Musselman Lake and Winsor Lake) and three land cover types: residential area, open area (grassland and woody area), and park and recreation. The residential area consists of single detached dwellings with mature street and backyard trees planted at least ten years ago. There are different types of trees that live in the study area, including deciduous trees such as maple, ash, oak, elm, black cherry, basswood, and conifers.

Two mLiDAR datasets were acquired by Titan on July 2, 2015, which had two flight lines that covered and intersected at the study area. The flight altitudes were above 1000 m with a pulse frequency of 100 kHz for each channel, yielding an average point spacing of 0.8 m per point and an average point density of 7.7 point/m².

Field data were collected on February 9, 2016 (see Fig. 1). A total of 40 trees were sampled in the field that contained four attributes; height, DBH, crown diameter, and biomass were recorded for each single tree. Tree heights were measured using a hypsometer in units of meter. DBH was measured with a diameter tape in units of centimeter. Since the field measurement was conducted during the leaf-off season, the third attribute, crown diameter, was measured using aerial photographs from Google Earth. The crown diameter is defined as the mean of the maximum crown diameter and the diameter measured at the direction perpendicular to the maximum, using the Ruler tool in Google Earth in units of meter. The fourth attribute, single tree carbon storage, is estimated by plugging the field-measured DBH and tree height into the Canadian national aboveground all-

species biomass equations (Lambert et al., 2005). The equations calculate the dry aboveground biomass by relating tree height and DBH to each biomass component, such as wood, bark, and foliage, with a uniform relationship: $Biomass = \beta_1 DBH^{\beta_2} H^{\beta_3}$; where β_1 , β_2 and β_3 are the parameters generated for the all-species group with different values according to the tree compartments. The carbon storage in sampled trees was then defined as half of the sum of the dry aboveground biomass in each compartment.

3. METHOD

3.1 mLiDAR data processing

After removing outliers and rectifying the mLiDAR intensity values, point clouds from two flight strips were merged together; in total, three mLiDAR point clouds were acquired by the Titan laser channels. Then each point cloud was rasterized into an intensity image with a ground resolution of 1m. The pixel size was selected according to the point spacing of the dataset. By selecting the pixel size close to the point spacing, most of the pixels can contain at least one point, and the vertical distribution of the points can be largely highlighted. In this way, points were grouped into 1 m grids and the pixel values were assigned by the mean intensity of the points within the grid. For the grids which had no point filled in, the grid values were interpolated linearly by searching the neighbors. Here, three mean intensity raster data were generated for channel 532 nm, 1064 nm, and 1550 nm, respectively.

Besides the generation of mLiDAR intensity images, DSM and DTM were created from the raw mLiDAR by a ground-point filtering and rasterization process. The whole mLiDAR dataset was then classified into ground and non-ground classes. DTM raster data was generated by rasterizing all the ground points into 1m grids, based on the linear interpolation method. The DSM was generated in a similar way by using the non-ground class, and the maximum height within the grid was assigned to the pixel values. In this way, the points that represented the treetops could be largely reserved. Lastly, normalized DSM (nDSM) raster data was acquired by subtracting the DTM from the DSM.

3.2 Vegetation isolation

Besides the multispectral intensity and nDSM data described above, two additional indices were derived as follows:

$$pNDWI = \frac{C_{Green} - C_{NIR}}{C_{Green} + C_{NIR}} \quad (1)$$

$$pNDVI = \frac{C_{NIR} - C_{SWIR}}{C_{NIR} + C_{SWIR}} \quad (2)$$

where C_{Green} , C_{NIR} , and C_{SWIR} refer to the laser channels at 532 nm, 1064 nm, and 1550 nm, respectively.

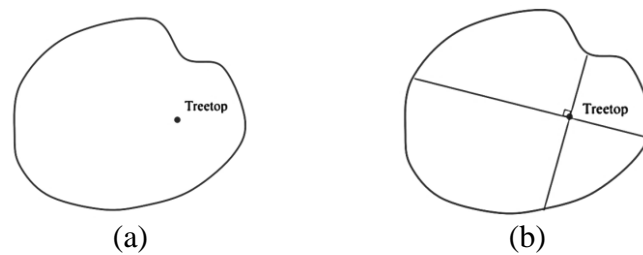


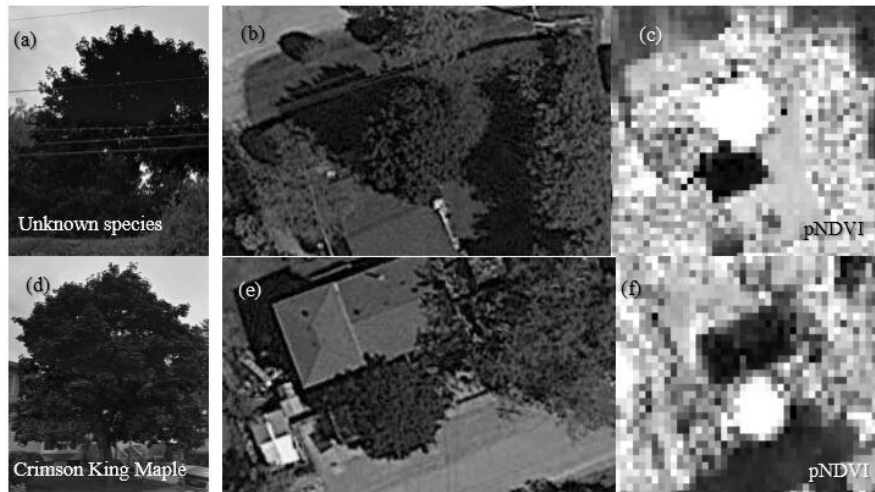
Fig. 3 Measurement of tree height and crown diameter: (a) location of the pixel with the maximum value within a tree crown; (b) illustration of the crown diameter measurement

By visually examining the pNDWI and pNDVI indices (see Fig. 2), both the pNDVI and pNDWI showed good discrimination for artificial objects. These two indices can facilitate the manual selection of training samples and work as the ancillary data in the classification process. The contribution of these two indices to the overall classification accuracy was analyzed. A total of six input data, including 1) Green channel intensity, 2) NIR channel intensity, 3) SWIR channel intensity, 4) nDSM, 5) pNDWI, and 6) pNDVI, were generated and input into the classification scheme.

Because the study area was characterized by simple residential landscape, it could be grouped into six land cover types, including water, house, road, grass, tree, and open area. However, due to the bathymetry capability of the channel at 532 nm, water points in the study area tended to have irregular intensity that was induced by the interaction of laser points with both the water surface and organic matter underneath. Hence, water bodies including Musselman Lake, Windsor Lake, and one small water region were masked out of the dataset, resulting in only five land cover types being trained and classified in this study. Interpreting land cover types from LiDAR intensity was not as easy as from passive optical images. Certain land cover types, such as grass and open area, could be distinguished from only one or two intensity data and could hardly be identified from the rest.

A support vector machine (SVM) classifier was selected to perform land cover classification with mLiDAR-derived data due to the popularity of SVM in single-channel LiDAR-related classification studies, making the classification result of this study comparable to previous studies. The SVM classification was performed on three combinations of the input data, shown in Table 1. The selection of input data was mainly designed for showing the benefits of mLiDAR in land cover classification (Selection 2), compared with single-channel LiDAR data (Selection 3). Meanwhile, Selection 1 was designed to examine the contribution of multispectral-intensity-derived indices in overall classification accuracy.

3.3 Dendrometric parameter estimation



(a)(b)(d), and (e) reprinted from Google Earth (2015)
Fig. 4 Trees with dark-colour leaves in Google Earth and the pNDVI

The tree-isolated nDSM was also referred to as the CHM, a model displaying tree positions by tree crowns in a top-down view and storing the height values in pixels. A 3×3 local maxima filter was first employed on the CHM to detect treetops. A pixel with the highest value amongst its eight neighbors was defined as the treetop. To eliminate the commission errors associated with the local maxima filtering and detect the true treetop pixels, the local maxima in the CHM were further filtered by the mLiDAR intensity data. The mLiDAR intensity values were dependent not only on the reflectivity of the object, but also on the range between the sensor and the object. A true treetop pixel would have both high intensity and height values. Under this assumption, another 1-m raster data was generated as the sum of the maximum intensity of the first return in each channel. The clusters of local maxima in the CHM which had more than fifteen pixels together were further extracted, and only the pixels that were also the local maxima in the maximum intensity layer were retained in the final treetop results. Previous studies relied on changing the window size and shape of the filter to refine the treetops (Chen et al., 2006; Zhao et al., 2009). These approaches were not suitable here because the CHM resolution (1 m) generated in this study was relatively coarse, so that increasing the window size of the local maxima filter would result in excluding small tree crowns.

The Marker-controlled watershed segmentation was applied to segment the CHM into individual tree crowns by defining the pre-detected treetops as the markers. In this way, every pre-detected treetop would have one closed segment. The performance of the segmentation in isolating tree crowns was evaluated by the absolute accuracy, calculated as:

$$\text{absolute accuracy}_{\text{tree isolation}} = \frac{n_{1,1}}{n_{\text{total}}} \quad (3)$$

where $n_{1,1}$ is the number of detected crown segments which have a one-to-one relationship to the ground truth; n_{total} is the number of tree crowns in the ground truth. Tree height is defined as the average of the local maxima within each segment, and crown diameter is defined as the average of the maximum crown diameter passing through the center of the local maxima and the one measured at the perpendicular direction (see Fig. 3).

To evaluate the accuracy of the mLiDAR-derived dendrometric parameters, the mLiDAR-derived tree height and crown diameter were compared with the field measurements. The crown segments generated from the LiDAR data were matched with the 40 field-sampled trees, and the RMSE and bias were calculated to compare the mLiDAR-derived dendrometric parameters with field samples:

$$\text{Bias} = \frac{\sum_{i=1}^n X_{ALS,i} - X_{field,i}}{n} \quad (4)$$

$$\text{RMSE} = \sqrt{\frac{\sum_{i=1}^n (X_{ALS,i} - X_{field,i})^2}{n}} \quad (5)$$

$$\text{RMSE}\% = \frac{\text{RMSE}}{\bar{X}_{ALS}} \quad (6)$$

where n is the number of field samples, which equaled 40 trees in this study; X refers to the values of dendrometric parameters (height or crown diameter) measured either in the field or from the ALS data; and \bar{X}_{ALS} is the arithmetic mean of the mLiDAR-derived measurements. Moreover, a linear regression model was fit to the mLiDAR-derived tree height and crown diameter to determine if there was a strong correlation between these two variables.

3.4 Carbon storage modeling

In order to predict the carbon storage in trees, a multiple linear regression model was developed empirically to fit the data, with the LiDAR-derived dendrometric parameters as the independent predictors and the field-measured DBH as the predicted variable. The empirical equation derived from the LiDAR-DBH linear regression model has the form:

$$\text{DBH}_{Field} = a \cdot \text{CD}_{ALS} + b \cdot H_{ALS} + c \quad (7)$$

The 40 field-sampled trees were split into two datasets, with 20 trees used for model parameterization and the remaining 20 trees reserved for validation. To eliminate the influence of tree locations in model fitting, each 10 adjacent tree samples were grouped together under one sampling location, resulting in a total of four sampling groups. Six combinations of training and validation datasets were chosen by selecting two sampling locations out of four for model development and using the remaining two locations for validation. All six models were developed at a 0.05 significance level and were fitted through a cross validation process. The parameters generated for each model were collected. The predictive power of the regression models and the performance were inspected by the coefficient of determination (R^2), and the accuracy of the prediction was examined by the RMSE of the predicted parameters. Comparing R^2 and RMSE of the six mLiDAR-DBH regression models, the one with high R^2 in the model fitting and low RMSE in the validation was selected to predict DBH.

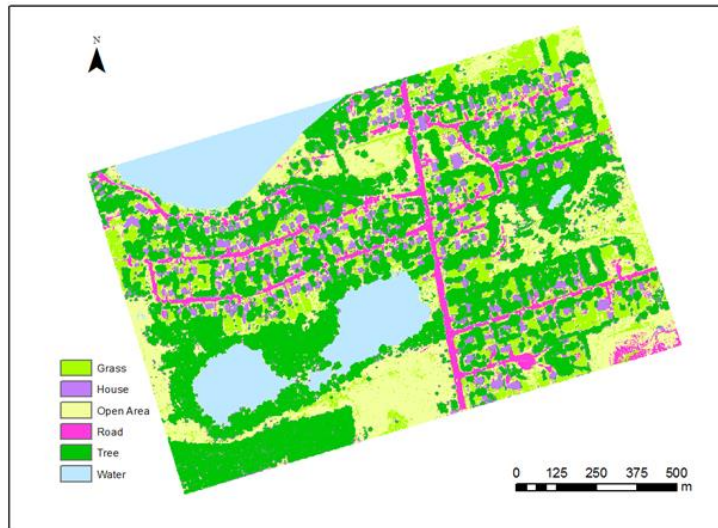


Fig. 5 Classification map

After selecting the mLiDAR-DBH regression model, the mLiDAR-estimated DBH and height were plugged into the Canadian national above-ground biomass equations proposed by Lambert et al. (2005) to estimate the carbon storage in trees. From Lambert et al. (2005), the set of equations based on DBH and height for all species was selected to calculate the biomass, since no genus or species information was available in this study. The above-ground biomass was estimated as the sum of biomass in tree compartments (foliage, branch, wood, and bark). The carbon stored in trees was estimated as the half of total biomass. The carbon storage predicted by the mLiDAR-derived parameters was compared with that estimated by the field-measured DBH and height and evaluated by the RMSE and R^2 .

To show whether carbon storage in trees varied with land cover types, the mLiDAR-derived tree-crown segments were first converted into vector data in GIS, with the amount of carbon storage stored in the attributes. The carbon storage within each land cover type was calculated by adding up all the carbon storage in trees and dividing by the area of the land cover type. For the Town of Whitchurch-Stouffville, the carbon stocks were extrapolated by multiplying the specific carbon amount per unit area with the total area of each land cover type. For those land cover types which were excluded in the study area (namely government and institutional areas and industrial sites), the carbon stored in government and institutional areas was given the same amount per unit area as the residential, but the carbon stored in industrial sites was given zero. Then a citywide carbon storage map was created.

4. RESULTS AND DISCUSSION

4.1 Analysis of Multispectral LiDAR Data for Land Cover Classification

Table 2. Validation statistics for the mLiDAR-derived dendrometric parameters

Parameter	RMSE	RMSE%	Bias	Bias%
Height (m)	1.21	6.8%	-0.20	-0.1%
Crown Width (m)	1.47	16.4%	-0.18	-2%

Table 3. Results of model fitting and model validation

Mode l	Model Fit R ²	Model Fit RMSE (cm)	Validation R ²	Validation RMSE (cm)
1	0.83	5.35	0.80	6.82
2	0.86	6.60	0.76	5.60
3	0.86	3.86	0.71	8.25
4	0.75	7.89	0.77	4.82
5	0.78	5.59	0.85	6.55
6	0.81	7.00	0.83	5.20

Table 4. Accuracy of mLiDAR-predicted vs. field-measured results

Parameter	RMSE	RMSE%	Bias	Bias%
DBH (cm)	6.39	13.1%	0.44	0.1%
Carbon (kg)	142.0	28.6%	14.4	2.9%

Because the classification at tree-genus or -species level is important, especially for precise biomass estimation, the spectral patterns of the tree class were examined further to find if current mLiDAR datasets could distinguish the tree class into conifer and deciduous trees. After confirming the tree types in Google Earth, there were no obvious distinctions between the tree genus by visual observations. However, through close visual observation of the pNDVI dataset, the trees with dark-colour leaves, such as the Crimson King Maple tree, could stand out from the tree class (see Fig. 4). The mLiDAR datasets generated in the chapter may not be sensitive enough to provide separate classification for conifers and deciduous trees. However, the analysis presented here shows that the mLiDAR intensity may be influenced by factors such as the colour/reflectivity of the objects, which in turn will be beneficial to studies of tree mortality, rooftop solar energy, and so on.

Accuracy assessment was conducted on the classification results in order to examine the classification performance of mLiDAR data. Fig. 5 shows the final classification map. The combination of all six input data achieved the highest overall accuracy among the three selections. The 89% overall accuracy was achieved using the mLiDAR-derived raster data, which indicated that the contributions of the two calculated indices to the overall accuracy were not significant. The comparison between single-channel LiDAR data and mLiDAR data on land cover classification was also conducted; the same classification process was applied to the nDSM and NIR bands only. The overall accuracy of classification in use of single-channel LiDAR data was around 79%.

4.2 Results for the Local Maxima Selection

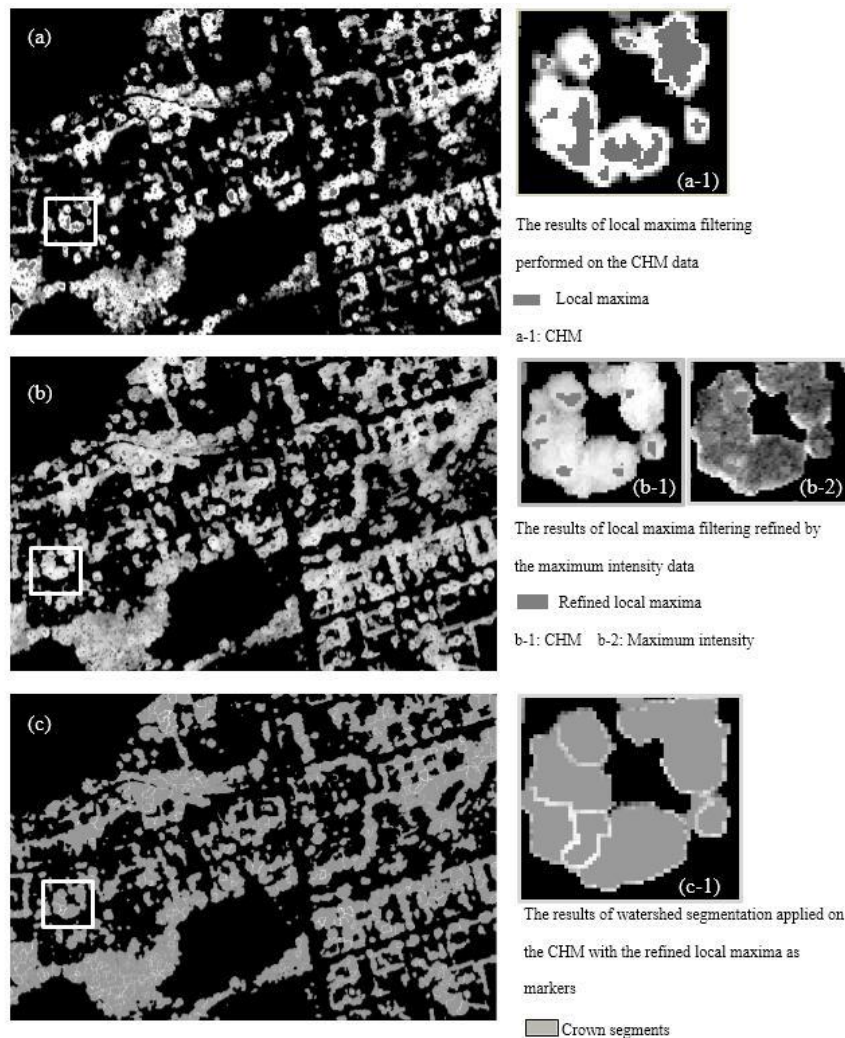


Fig. 6 Results obtained by local maxima filtering and the marker controlled watershed segmentation

The second step of the methodology was to find the local maxima in the tree-isolated nDSM (the so-called *CHM*) as the treetop candidates. In this paper, a new approach is proposed to reduce the number of pixels generated by the original 3×3 local maxima filter and to find the true treetop pixels. Fig. 6 illustrates the comparison between the original local maxima result performed on the CHM and the refined result, which only retained the pixels that had a local maximum on both the maximum intensity data and the CHM. The clusters of local maxima in the original result were eliminated by the proposed method. Then the watershed segmentation algorithm was applied to generate crown segments, using the refined local maxima as the markers (see Fig. 6 (c)).

4.3 Validations for the ALS-derived Dendrometric Parameters

The accuracies of LiDAR-derived tree height and crown width were assessed by the samples measured in the field. For the mLiDAR-derived tree height, an RMSE of 1.21 m (relative RMSE = 6.8%) and a negative bias of 0.2 m (relative bias = -0.1%) are given in Table 2. For the LiDAR-derived crown width, an RMSE of 1.47 m (relative RMSE = 16.4%) and a negative bias of 0.18 m

(relative bias = - 2%) were observed. The tree height was underestimated because of the undergrowth and factors related to the flight height (1000 m) and the point density (7 to 8 points/m²). The relative RMSE of crown width was mainly caused by the resolution of the CHM and the results of crown segmentation.

4.4 Validations for the mLiDAR-predicted DBH and Tree Carbon

The results of model fitting and validation of the six mLiDAR-DBH regression models are listed in Table 3. The 40 field-measured samples were previously split into 4 groups, with 10 trees in each group. The models were iteratively fitted by 20 trees selected from two groups out of four and were validated by the remaining 20 trees. Model 2 was selected as the overall best model to predict DBH in this study because it has a relatively high coefficient of determination ($R^2=86\%$) from model fitting and a relatively low RMSE (5.6 cm) from the validation. The regression equation is:

$$DBH = -11.2792 + (-0.2958) \times CD + 3.2637 \times H \quad (8)$$

To determine the number of decimal places for the coefficients in the regression equation, the residuals between the DBH values predicted by the coefficients with eight decimal places and those predicted by coefficients rounded to two, three, and four decimal places, respectively, are compared in Fig. 8. To keep high prediction accuracy, coefficients in the regression model are rounded to four decimal places. Moreover, the R^2 between field-measured tree height and crown width was calculated as 0.34, indicating insignificant correlation between these two variables. Though DBH cannot be directly measured on the CHM, all the generated mLiDAR-DBH models showed that the DBH correlated well with mLiDAR measurements. The accuracies of the mLiDAR-modeled DBH and mLiDAR-derived carbon storage are given in Table 4. The predicted DBH using mLiDAR-derived parameters corresponded to an RMSE of 6.4 cm (relative RMSE = 13.1%) and a bias of 0.4 cm. The relationship between field-measured DBH and mLiDAR-modeled DBH is plotted in Fig. 8. The results are compared with the reference carbon storage estimated by field-measured DBH and plotted in Fig. 9. The R^2 of both DBH and carbon storage were both above 0.80. The predicted carbon storage using ALS-modeled DBH corresponded to an RMSE of 142 kg (28.6%) and a bias of 14.4 kg.

4.5 Analysis of the LiDAR-estimated Results

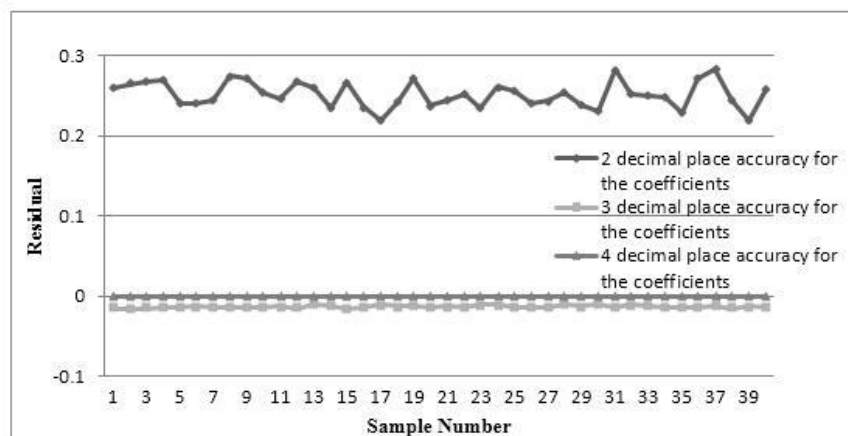


Fig. 7 Residual plots for model-predicted DBH generated by coefficients with 2, 3, and 4

decimal places
3D Modeling of Urban Tree Crown Volumes Using Multispectral LiDAR Data (8875)
Jonathan Li (China, PR) and Xinqu Chen (Canada)

FIG Working Week 2017

Surveying the world of tomorrow - From digitalisation to augmented reality

Helsinki, Finland, May 29–June 2, 2017

The accuracy of tree-height measurements using LiDAR data has previously been studied by Yu et al. (2004), Kaartinen et al. (2012), and Hadaś & Estornell (2016). Yu et al. (2004) found that as flight altitude increased from 400 m to 1500 m, the accuracy of tree heights lowered from 0.76 to 1.16 m for single tree species. Kaartinen et al. (2012) reported that the best methods which utilized the local maxima finding with a point density of 8 points / m² could obtain a RMSE of 60 cm to 80 cm for tree heights. Hadaś & Estornell (2016) showed that the bias of tree height measurements could decrease from -1.48 m to -0.72 m if the point density increased from 3.5 points / m² to 9 points / m². The RMSE achieved in the present study is in line with these studies and is potentially affected by the errors generated during the field measurements. Both overestimations of the crown size and underestimations of the tree heights are likely a result of the overlaying crown covers of the dominant tree and the suppressed trees, but could be mitigated if the resolution of CHM is at the sub-meter level. The results of LiDAR-modeled DBH are in line with the findings in Hauglin et al. (2014) and Popescu et al. (2007) regarding the tree height and crown diameter as good predictors to predict DBH using linear regression. The accuracy found in the present study is higher than these two studies. Hauglin et al. (2014) reported an RMSE of 35% for LiDAR-estimated DBH of Norway spruce. Popescu et al. (2007) reported a lower RMSE (4.9 cm) and higher R² compared to the present study. However, considering that the accuracies in Popescu et al. (2007) were for single tree species, which had an average DBH of 29.55 cm, and that they used all 43 sampled trees to construct the model and validate the model using the same dataset, the RMSE% and R² in their study would understandably be higher than that in this study. For aboveground biomass, Popescu (2007) reported an RMSE of 47% for single tree species. Kankare et al. (2013) reported RMSEs of 26.3% and 36.8% for pines and spruce, respectively. Huaglin et al. (2014) achieved an RMSE of 35.1% for biomass estimation. Though the achieved accuracy of carbon estimation is higher in the present study, these studies are not entirely comparable because some studies used field-destructive measurements as reference data, which were not available in this study. Also, because genus information is not available, the estimation of carbon stocks was done by the allometry equations for all species in Lambert et al. (2005), so that the derived carbon mainly depended on the LiDAR-derived DBH and height, with little consideration given to the differences in species.

4.6 Analysis of the Carbon Storage

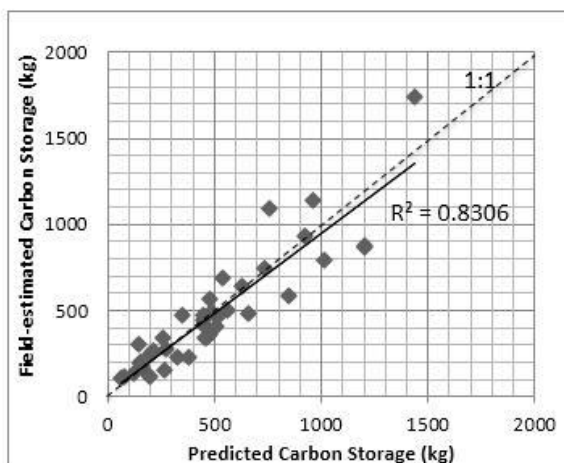


Fig. 8 Scatterplot of the LiDAR-modeled vs. field-measured DBH.

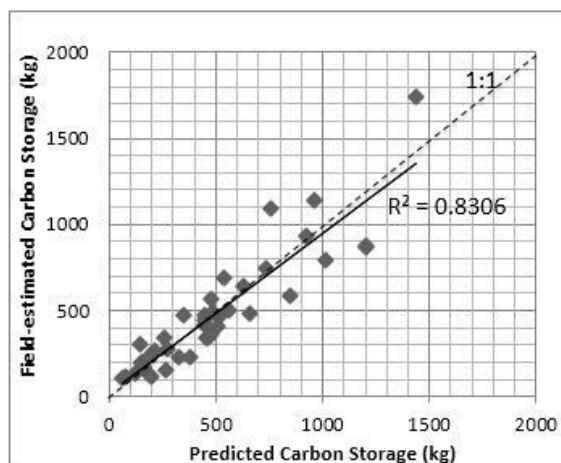


Fig. 9 Scatterplot of the LiDAR-predicted vs. field-estimated carbon storage.

3D Modeling of Urban Tree Crown Volumes Using Multispectral LiDAR Data (8875)
Jonathan Li (China, PR) and Xinqu Chen (Canada)

FIG Working Week 2017

Surveying the world of tomorrow - From digitalisation to augmented reality

Helsinki, Finland, May 29–June 2, 2017

There were a total of 2555 dominant trees in the study area. The trees were located along the roadsides, in the backyards, and around the lakes. The average tree carbon was 484.3 kg and resulted in a total of 1.24 kt C (10^3 tons Carbon). The study area could be divided into four land use types: residential, park and recreational, open area, and water. The open area occupied the largest portion of the study area, 47.0 ha. The residential area occupied 25.8 ha. The park had a small area of 2.5 ha. The extracted carbons in trees were therefore grouped based on the land use type, and the amount of carbon stored in each land cover type was calculated. Within the study area, the open area contained the largest tree carbon stocks (682.7 t), followed by the residential area (362.6 t), and finally the parks and recreational area (29.2 t). The tree carbon storage for the open area, residential area, and parks on a per-unit-area basis were 14.54 t C/ha, 14.08 t C/ha, and 11.57 t C/ha, respectively. City wide, open area occupied 83.7% (191.5 km²) of the total city area and contained the largest carbon storage, 278.4 kt C. Residential area covered 8.3% (19.4 km²) of the total city area and contained 27.3 kt C tree carbons. Parks covered 12.8 km² with a total carbon storage estimated at 14.8 kt C. The carbon storage map shows that large tree carbon stocks are accumulated in urban environments and are distributed heterogeneously among land use types (see Fig. 10).

The estimated tree carbons in the study area were in line with the estimation of carbon storage in Canadian urban trees conducted by researchers at Environment Canada (Pasher et al., 2014). Pasher et al. (2014) estimated the carbon stocks in trees by applying the crown cover area of urban trees and a Canadian-specific area-based growth rate for urban trees. Pasher et al. (2014) reported a total urban area of 5317 km² in Ontario Mixedwood Plains with an estimation of carbon storage at 9177.6 kt C, resulting in a carbon storage per unit urban area as 17 kt C/ha. This is slightly more than what has been predicted in this study (around 14 kt C/ha).

5. CONCLUSIONS

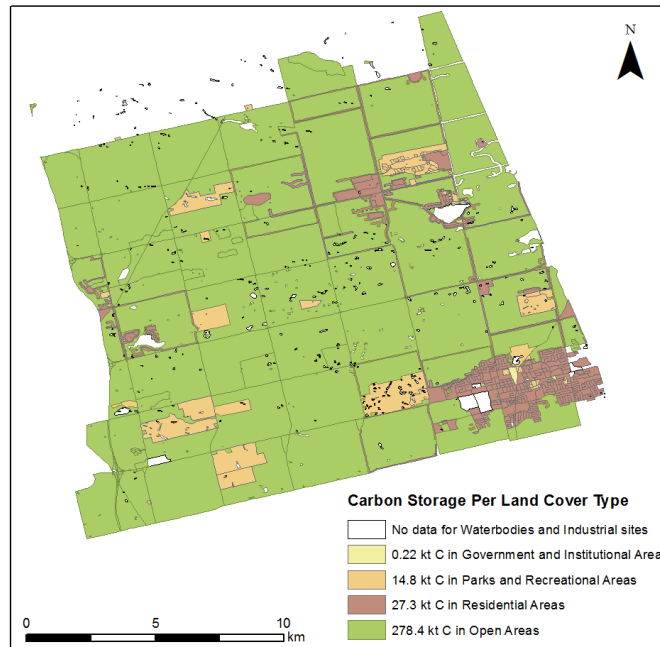


Fig. 10 Carbon storage map for the Town of Whitchurch-Stouffville, Ontario

In this paper we have proposed a method to map land covers and estimate aboveground carbon storage in trees at a spatial resolution of 1 m using mLiDAR data. Our study achieved an overall accuracy of 90%, which was 11% higher than that obtained using single-wavelength LiDAR data. The dendrometric parameters at single-tree level can be derived directly from the mLiDAR data. It also shows how the use of both spectral and geometric properties of mLiDAR data can improve the detection of treetops. This paper presented the feasibility of applying forest-based allometric methods to assess carbon stocks in urban environments. Dominant trees with fewer underneath or nearby trees were better detected and analyzed. Though DBH cannot be directly measured from mLiDAR data, the mLiDAR-predicted DBH remains a power predictor for estimating tree carbon at the individual-tree level. More accurate tree carbon measurements could be obtained if genus information and crown base heights were further investigated. An improvement of derivation of the crown width would also help in better prediction of tree carbon stocks. This paper derived similar carbon amounts per unit area in both residential areas and open areas within the study area, because the open area had twice the size of the residential area but the density of the canopy covers was less than it was in the residential area.

REFERENCES

- Berg, M. V. D., Wendel-Vos, W., Poppel, M. V., Han, K., Mechelen, W. V., and Maas, J., 2015. Health benefits of green spaces in the living environment: a systematic review of epidemiological studies. *Urban Forestry & Urban Greening*, 14(4), 806-816.
- Chen, Q., Baldocchi, D., Gong, P., and Kelly, M., 2006. Isolating individual trees in a savanna woodland using small footprint LiDAR data, *Photogrammetric Engineering & Remote Sensing*, 72(8), 923-932.

- Davies, Z.G., Edmondson, J.L., Heinemeyer, A., Leake, J.R. and Gaston, K.J. 2011. Mapping an urban ecosystem service: quantifying above-ground carbon storage at a city-wide scale, *Journal of Applied Ecology*, 48(5), 1125-1134.
- Donovan, G.H. and Butry, D.T., 2010. Trees in the city: Valuing street trees in Portland, Oregon. *Landscape and Urban Planning*, 94(2):77-83.
- Hadaś, E. and Estornell, J., 2016, Accuracy of tree geometric parameters depending on the LiDAR data density, *European Journal of Remote Sensing*, 49, 73-92.
- Hauglin, M., Dibdiakova J., Gobakken T., and Næsset. E., 2013. Estimating single-tree branch biomass of Norway spruce by airborne laser scanning, *ISPRS Journal of Photogrammetry and Remote Sensing*, 79, 147-156.
- Huang, Y., Yu, B., Zhou, J., et al. 2013. Toward automatic estimation of urban green volume using airborne LiDAR data and high resolution Remote Sensing images, *Frontiers of Earth Science*, 7(1), 43-54.
- Kaartinen, H., Hyyppä, J., Yu, X., et al. 2012. An international comparison of individual tree detection and extraction using airborne laser scanning, *Remote Sensing*, 4(4), 950-974.
- Lambert, M.C., C.H. Ung, and Raulier, F., 2005. Canadian national tree aboveground biomass equations, *Canadian Journal of Forest Research*, 35(8), 1996-2018.
- Lieth, H., 1963. The role of vegetation in the carbon dioxide content of the atmosphere, *Journal of Geophysical Research*, 68(13), 3887-3898.
- Popescu, S.C., Wynne, R.H., and Nelson, R.F., 2003. Measuring individual tree crown diameter with LiDAR and assessing its influence on estimating forest volume and biomass, *Canadian Journal of Remote Sensing*, 29(5), 564-577.
- Popescu, S.C., 2007. Estimating biomass of individual pine trees using airborne LiDAR, *Biomass and Bioenergy*, 31(9), 646-655.
- Raciti, S.M., L.R. Hutyrá, and J.D. Newell., 2014. Mapping carbon storage in urban trees with multi-source remote sensing data: Relationships between biomass, land use, and demographics in Boston neighborhoods, *Science of The Total Environment*, 500, 72-83.
- Roy, S., Byrne, J., and Pickering, C., 2012. A systematic quantitative review of urban tree benefits, costs, and assessment methods across cities in different climatic zones, *Urban Forestry & Urban Greening*, 11(4), 351-363.
- Sawka, M., Millward, A.A., Mckay, J., and Sarkovich, M., 2013. Growing summer energy conservation through residential tree planting, *Landscape and Urban Planning*, 113, 1-9.
- Schreyer, J., Tigges, J., Lakes, T., and Churkina, G., 2014. Using airborne LiDAR and QuickBird data for modelling urban tree carbon storage and its distribution — A case study of Berlin. *Remote Sensing*, 6(11), 10636-10655.
- Wichmann, V., Bremer, M., Lindenberger, J., Rutzinger, M., Georges, C., and Petrini-Monteferrri, F., 2015. Evaluating the potential of multispectral airborne LiDAR for topographic mapping and land cover classification, *ISPRS Annals*, 1, 113-119.
- Xu, T., Sathaye, J., Akbari, H., Garg V., and Tetali, S., 2012. Quantifying the direct benefits of cool roofs in an urban setting: Reduced cooling energy use and lowered greenhouse gas emissions, *Building and Environment*, 48, 1-6.
- Xu, Q., Hou, Z., Maltamo, M., and Tokola. T., 2014. Calibration of area based diameter distribution with individual tree based diameter estimates using airborne laser scanning, *ISPRS Journal of Photogrammetry and Remote Sensing*, 93, 65-75.

Yu, X., Hyypä, J., Kaartinen, H., and Maltamo, M., 2004. Automatic detection of harvested trees and determination of forest growth using airborne laser scanning, *Remote Sensing of Environment*, 90(4), 451-462.

Zhao, K., Popescu, S., and Nelson, R., 2009. Lidar remote sensing of forest biomass: A scale-invariant estimation approach using airborne lasers, *Remote Sensing of Environment*, 113(1), 182-196.

CONTACTS

Dr. Jonathan Li, Professor

Fujian Key Laboratory of Sensing and Computing for Smart Cities, School of Information Science and Engineering, Xiamen University, 422 Siming Road South, Xiamen 361005, CHINA, junli@xmu.edu.cn

Department of Geography and Environmental Management, University of Waterloo.
200 University Avenue West, Waterloo, ON N2L 3G1, CANADA, junli@uwaterloo.ca